Robust CCD photoelectric autocollimator for outdoor use

Min Gao (高 敏)[1,2], Zuoren Dong (董作人)[1*], Zhenglan Bian (卞正兰)[1,2], Qing Ye (叶 青)[1], Zujie Fang (方祖捷)[1], and Ronghui Qu (瞿荣辉)[1]

[1] *Shanghai Key Laboratory of All Solid-state Laser and Applied Techniques, Shanghai Institute of Optics and Fine Mechanics, Chinese Academy of Sciences, Shanghai 201800, China*

[2] *Graduate University of Chinese Academy of Sciences, Beijing 100049, China*

[*] *Corresponding author: zrdong@siom.ac.cn*

Received March 7, 2011; accepted March 31, 2011; posted online June 21, 2011

A robust charge-coupled device (CCD) photoelectric autocollimator for outdoor use is designed and demonstrated. The influence of outdoor conditions on the signal-to-noise ratio (SNR) and imaging quality of the measuring system is experimentally analyzed. The pulse width modulation technology is applied to the automatic feedback control of the actively regulated illuminating light source of the measuring system to maximize SNR while avoiding image saturation. A Fourier phase shift method for subpixel estimation is adopted to achieve high-accuracy measurement in the presence of noises. Experimental results indicate that the technologies proposed here largely improve the measuring stability, dynamic range, and accuracy of the CCD photoelectric autocollimator used outdoors.

OCIS codes: 120.0120, 120.1680, 100.0100, 100.2650.
doi: 10.3788/COL201109.091201.

A charge-coupled device (CCD) photoelectric autocollimator is an automated precision optical instrument for the non-contact measurement of small angles. It has broad applications in opto-mechanical alignment, angle measurement of prisms, and performance inspection of turntables, which are all conducted indoors. There are also many cases where autocollimators have to be used outdoors, such as in the straightness measurement of guideways and in the initial attitude determination before missile launches[1−3], which both require higher requirements.

Unlike the indoors, the outdoors can have a high temperature, which brings about big noises, or a low temperature, which decreases the charge transfer efficiency (CTE) of CCD[4]. Moreover, the quality of the optical surfaces can degrade due to the temperature, resulting in the distortion of image signal. Pollution on the light path and lens (e.g., rainwater, smog, and dust), lateral change in a relative position between the autocollimator and measured prism, and large measured angles, among others, can introduce image signal attenuation and even disappearance if there is no compensatory approach. The intensity fluctuation of the image signal exceeds the dynamic range of the CCD when it is used outdoors. Both the signal-to-noise ratio (SNR) and imaging quality are largely affected by the outdoor environment factors. The familiar subpixel algorithms used for improving the resolution of CCD are not immune to noises and distortion. They must be considered when developing an autocollimator for outdoor use, which is closely associated with measuring stability and accuracy.

Currently, the autocollimators reported in most papers are designed for indoor use. Many methods have been presented to obtain an ultra high accuracy of $0.005''$[5]. Commercially available autocollimators usually have an accuracy of $0.2''$, and the measurement ranges no more than $\pm 1\,000''$, making them unsuitable for outdoor use because their operation temperature is usually limited to 15−25 °C[6]. Even more rigorous measuring conditions are sometimes required to obtain the nominal accuracy. Although some papers have mentioned autocollimators for outdoor use, they do not include the research methods and experimental results[7,8]. Developing a compact and robust CCD autocollimator with a relatively large measuring range for outdoor use is practically necessary.

In this letter, we demonstrate a compact and robust CCD photoelectric autocollimator for outdoor use with commercial off-the-shelf components. The design parameters of the system are presented. The influence of the field conditions on the SNR and imaging quality of the measuring system is experimentally analyzed. The SNR of the image signal is maximized while avoiding image saturation using a pulse modulated illuminating light source with an automatic feedback controlled pulse-width, which is synchronous with the CCD exposure time. The Fourier phase shift (FPS) method for subpixel image locating with anti-noise property is adopted to improve the measuring accuracy[9−12]. Using these technologies, a one-dimensional CCD photoelectric autocollimator is developed for outdoor use with a large measuring range, fine stability, and high precision.

The principle of the CCD autocollimator is shown in Fig. 1. A slight alternation of angle θ between the optical axis of the autocollimator and the mirror under-test, whose normal is parallel to the optical axis initially,

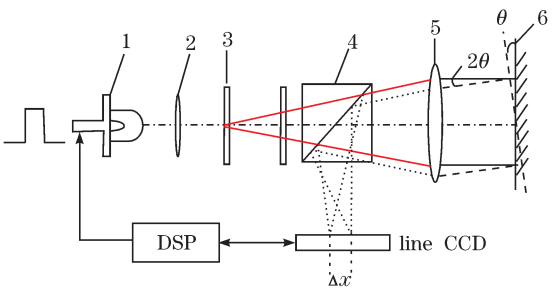

Fig. 1. Principle of the photoelectric autocollimator system. 1-LED; 2-collecting lens; 3-reticle; 4-light splitter; 5-object lens; 6-reflector.

can cause a deviation Δx of the reticle image on the line CCD[13]. If the focal length of the objective is f, according to the principles of geometric optics, the relationship between the deviation Δx and angle θ can be written as

$$\Delta x = f \times \tan 2\theta. \tag{1}$$

For small tilt angles, the image displacement Δx is proportional to θ. That is, the small angular displacement is transformed into a linear displacement of the reticle image.

As shown in Fig. 1, the autocollimator we developed consists of an optical conjugate imaging system, a line CCD, a high-light light emitting diode (LED), and an embedded control processing system based on the digital signal processing (DSP) unit. To obtain a compact design, the focal length of the object lens was 200 mm, with an effective optical aperture of 32 mm. The chosen CCD chip (TCD1501D, TOSHIBA, Japan) has 5 000 pixels, whose unit cell size is 7×7 (μm) and slit width is 50 μm. We can obtain the following equations:

$$\theta_{\text{resolution}} = \frac{1}{2}\arctan\left(\frac{\Delta X}{f}\right), \tag{2}$$

$$\phi = 2L \cdot \tan(2\theta_{\text{rang}}), \tag{3}$$

where $\theta_{\text{resolution}}$ is the theoretical measuring angle resolution without any subdivision technology, ΔX is the unit cell size of CCD, ϕ is the effective optical aperture, L is the measuring distance, and θ_{rang} is the angle measurement range.

The red LED with power of 2 W was chosen as the cold-light source to diminish the thermal distortion[13]. The control and processing unit was constructed based on DSP chip (TMS320F2812, Texas instrument, USA) with a clock rate of 155 MHz[14], which carried out the drive signals of the CCD, image capturing and subpixel locating, modulation signals on LED, and remote communication. A measuring speed of 200 Hz for the CCD photoelectric autocollimator was also ensured.

According to Eq. (1), when the focal length of the objective f is fixed, the measurement precision of angle θ depends only on the measuring accuracy of the deviation Δx. The SNRs of the image signals, imaging quality, and subpixel algorithm are the primary issues closely related to the image locating accuracy. A high-precision opto-mechanical system design must be guaranteed beforehand.

The SNR of the image decreases without any active compensatory approach when the CCD photoelectric autocollimator is used outdoors[15]. This is due to the field conditions (e.g., temperature, rainwater, smog, dust, etc.) or large deflection angles relative to the optical aperture, as we have analyzed in our previous publications[16]. The influence of high and low temperatures on the SNR of the image signal captured by the CCD is investigated by a simple 1:1 imaging system with a settled intensity of illumination placed in a temperature controller. As shown in Fig. 2, comparing the image signal at −40 °C with that at 60 °C, the dark current noise disappears at −40 °C, whereas that the image signal reaches 0.5 V with a low-frequency modulation at 60 °C. However, the amplitude of the signal at −40 °C

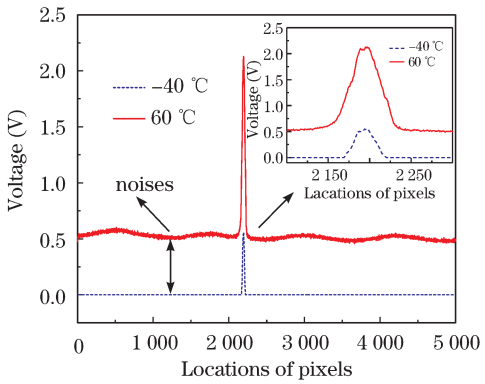

Fig. 2. Image signal at –40 and 60 °C.

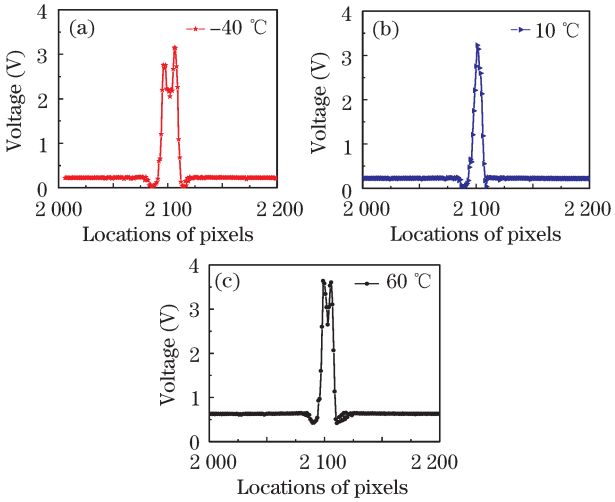

Fig. 3. Image signals of the autocollimator at temperatures of (a) −40 °C; (b) 10 °C; (c) 60 °C.

becomes one-third of that at 60 °C. The CTE of the CCD is considered to decline when the temperature is below its operating conditions. It becomes even worse if a large measured angle for the CCD autocollimator occurs simultaneously, as the flux loss is caused by the deflection of the measured mirror[16]. Similarly, pollution on the light path and lens can also cause flux loss, reducing the SNR further.

To investigate the influence of high and low temperatures on the imaging quality of the measuring system, the autocollimator was placed in the temperature controller. The image signal was obtained when the temperature changed from −40 to 60 °C. Figure 3 shows the image signals of the autocollimator with ambient temperatures at −40, 10, and 60 °C. The distributions of the images become bimodal and asymmetric when the temperatures are at −40 and 60 °C. In practice, this begins to occur when the temperature is below −20 °C and above 30 °C. The decrease in accuracy of the beam splitter, as shown in Fig. 1, is considered the main cause of imaging distortion.

Currently, the precision of the most commonly used subpixel algorithms reported, such as centroid estimation and Gaussian fitting, is sensitive to noises and distributions of the signals, resulting in a non-ideal measuring

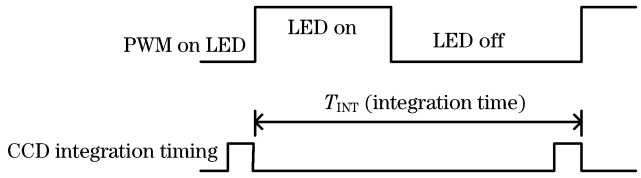

Fig. 4. PWM signal on LED.

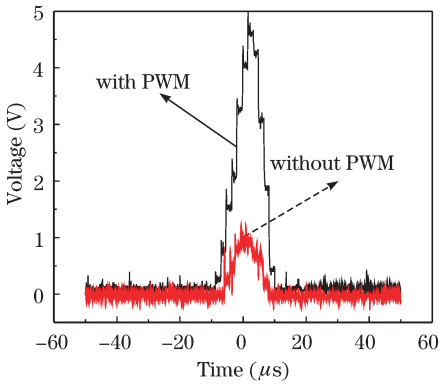

Fig. 5. Image signal obtained with and without PWM technology when the mirror deflects for 1°.

accuracy[17,18]. As a result, solving these problems with the development of a practical CCD photoelectric autocollimator for outdoor use is inevitable.

To acquire a good SNR of the image signal when it is attenuated by a light path (e.g., liquid), low temperature, and a large deflection angle relative to the small optical aperture, the light flux returning to the autocollimator is controlled by lighting time. As shown in Fig. 4, the pulse width modulation (PWM) signal on the LED is calculated and regulated from the peak intensity of the prior frame image by a digital proportinal-integral controller implemented on DSP, which is synchronous with the CCD exposure time. The amplitude of the image signal integrated by the CCD is related to the lighting time of LED during the integration period, which can be actively controlled according to specific circumstances to maximize the SNR while avoiding image saturation. Figure 5 shows the image signal captured by the CCD with and without the PWM technology when the mirror under test deflects for 1°. This indicates that the SNR is improved for about 5 times when the PWM technology is used. This method is superior to the regulation of the integration time of CCD, which also strengthens background noises and confines the range of choice of CCD chips. Another advantage of the active regulation of LED is that the dark current noises under different operating circumstances, as shown in Fig. 2, can be evaluated before the LED is on and subtracted as a background. The SNR improves because the background noises are separated from the image signal to a certain extent. As a result, the PWM technology introduced enlarges the dynamic range of the CCD autocollimator while maintaining a high SNR.

Aside from the SNR of the image signal, the light spot image locating precision is also related to the measuring accuracy of the CCD photoelectric autocollimator, especially when under noises and distortion. The sub-

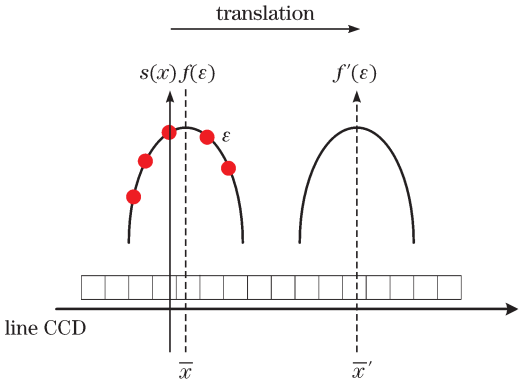

Fig. 6. Ideally sampled signal on the CCD.

pixel subdivision technology is one of the effective solutions to improve the fixed and limited resolution of the CCD[19,20]. The FPS proposed relies on the properties of the phase shifting of the Fourier transform; i.e., the information of the displacement in the time domain can be reflected in the phase spectrum. Analyzing the phase spectrum, the relationships between the two phase spectra of the sequence images can be found, and the displacement can be estimated by calculating the difference of the two phase spectra. Many methods for phase difference measurement have been reported[21,22]. However, in this letter, we introduce the "best symmetry center" method[23,24]. As shown in Fig. 6, a light spot imaging on the CCD can be considered a continuous waveform, which is sampled by the pixels of the CCD in the space domain. Ideally, the imaging signal acquired in our system is a symmetrical bell-shaped type with a limited bandwidth.

According to the properties of the Fourier transform, a real and even function similar to the symmetrical waveform $f(\varepsilon)$ shown in Fig. 6, which refers to its center of symmetry, necessarily has a zero argument $\phi_{F(s)} \equiv 0$ over all the frequency domains. The pixel of the peak of the sampled image is now chosen as the new origin of coordinates. The image signal can be expressed as $s(x)$. The relationship between $f(\varepsilon)$ and $s(x)$ can then be written as

$$s(x) = f(\varepsilon + \bar{x}), \tag{4}$$

where $\bar{x}$ represents the symmetrical center of $f(\varepsilon)$. The Fourier transform $s(\omega)$ of $s(x)$, and the Fourier transform $F(\omega)$ of $f(\varepsilon)$ follow the relations:

$$s(\omega) = \exp(\mathrm{j}\omega\bar{x})F(\omega), \tag{5}$$

$$\Delta\phi_{s(\omega)} = \phi_{s(\omega)} = \omega\bar{x}. \tag{6}$$

Thus, $\bar{x}$ can be estimated from each independent $\phi_{s(\omega)}$. The phase value $\phi_{s(\omega)}$ can be obtained by discrete fourier transform (DFT) on the sampled image signal $s(N)$, which is sampled from $s(x)$ by N points and centered on the pixel of the peak of the sampled image. Here, we present a simpler method that can be implemented easily on DSP. Based on experience, most noises occur at a high frequency[25]. The phase shifting of the fundamental frequency is chosen to calculate the translation for both

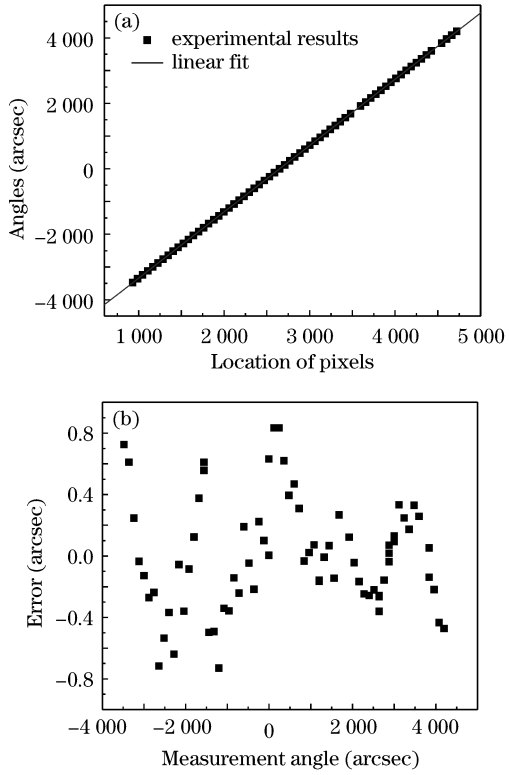

Fig. 7. (a) Linear relationship between the location of the pixels and measuring angles; (b) angle measurement error.

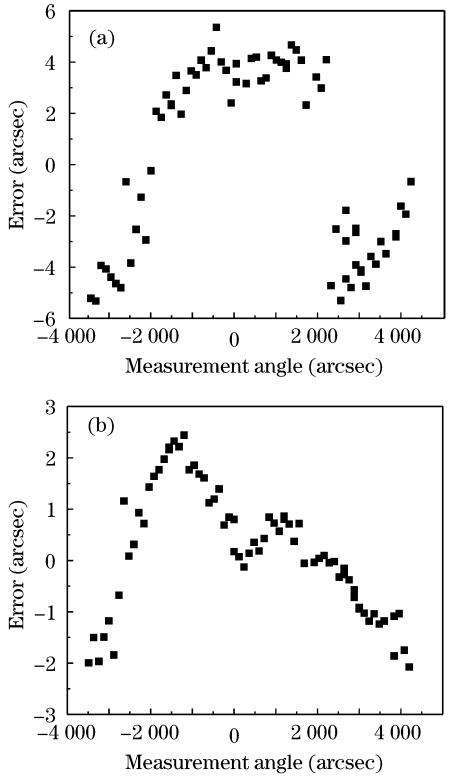

Fig. 8. (a) Accuracy of the centroid estimation; (b) accuracy of the Gaussian fitting.

high-precision and concise computation. The phase value $\phi_{s(\omega)}$ can then be obtained by calculating the arctangent of the ratio of the imaginary part to the real part of $s(\omega_0)$, resulting in the estimation of $\bar{x}$ with the following subpixel:

$$\phi_{s(\omega_0)} = -\tan^{-1}\left\{\frac{\mathrm{Im}[s(\omega_0)]}{\mathrm{Re}[s(\omega_0)]}\right\}, \tag{7}$$

$$\mathrm{Im}[s(\omega_0)] = \frac{1}{N}\sum_{i=1}^{N} s(i)\sin\left(\frac{2\pi}{N}\cdot i\right), \tag{8}$$

$$\mathrm{Re}[s(\omega_0)] = \frac{1}{N}\sum_{i=1}^{N} s(i)\cos\left(\frac{2\pi}{N}\cdot i\right). \tag{9}$$

The FPS method eventually provides the "best symmetry center" $\bar{x}$ of the signal, which is used as the feature point of the image. Compared with other subpixel algorithms that have been reported and are commonly used in CCD photoelectric autocollimators, the FPS algorithm is more insensitive to the direct current offset perturbation and low-frequency noise, which operates as a bandpass filter[26]. Hence, it is more tolerant to the symmetry of the signal, which is usually destroyed by the high-frequency parts. The random noise signal $n(x)$, which causes the phase estimation error $\Delta\phi(\omega)$, can be expressed as

$$\Delta\phi(\omega) \leqslant \arctan\frac{|N(\omega)|}{|F(\omega)|}. \tag{10}$$

Aside from a high SNR of the signal obtained using the PWM technology for a bell-shaped signal, the fundamental component contributes to the majority of the image signal, resulting in the high-precision phase estimation and position locating becoming the phase-shifting error. The other experimental noises that appear at other frequency components are also eliminated.

Thus, the FPS subpixel algorithm is suitable to be applied to the CCD photoelectric autocollimator for outdoor use. The measuring errors caused by background and high-frequency noises, which produce images distortion, are all reduced due to the intrinsic properties of the algorithm, where only the fundamental frequency of the image signal is selected for calculation.

With an accuracy of ±1 μrad, a laser autocollimator called laser diode sensor (LDS), was used to calibrate the precision of the photoelectric autocollimator we developed. A double side mirror attached to a turntable was placed between the LDS and the autocollimator, with the autocollimator 0.5-m away from the mirror. Initially, the normal of the mirror was adjusted parallel to the optical axis of the autocollimator. Rotating the mirror step by step, the angle value measured by LDS and the image signals captured by the CCD in the photoelectric autocollimator were simultaneously recorded. The relationship between the location of the pixels and measuring angles was acquired, as shown in Fig. 7(a). Comparing the angles measured by LDS and calculated by the CCD photoelectric autocollimator using the FPS method, the accuracy of the measurement system was obtained, as shown in Fig. 7(b). A measuring accuracy of $\pm1''$, with a measuring range of $\pm3\,600''$, was achieved.

The commonly used subpixel algorithms, namely, the centroid and the Gaussian fitting, were also implemented in the above calibration experiment for comparison. As shown in Fig. 8, the accuracy of the centroid estimation is $\pm6''$, whereas that of the Gaussian fitting reaches $\pm3''$

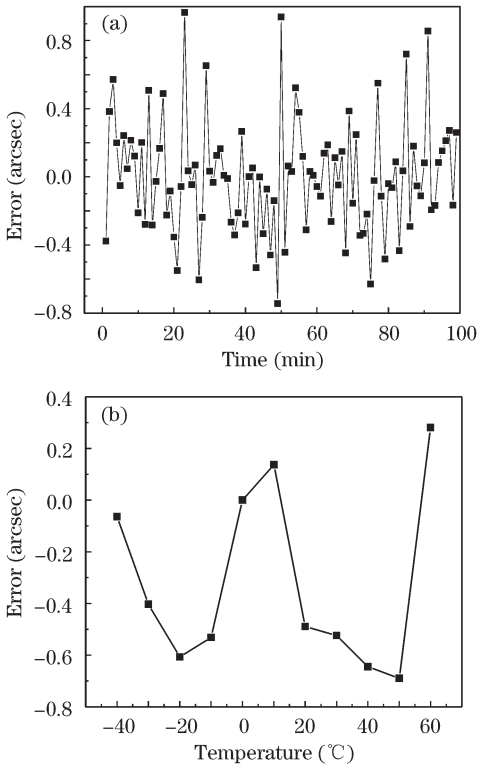

Fig. 9. Drift of the CCD photoelectric autocollimator. (a) Long-term drift; (b) drift versus temperature.

with a more complicated computation. The FPS method is more robust than the others, with a moderate computing complexity.

We then evaluated the drift performance with long time and temperature. Bounding a corner cube in the beam output port of the CCD photoelectric autocollimator, we obtained a measuring angle every minute for 100 min when the ambient temperature was 10 °C. Figure 9(a) shows the long-term drift of the CCD photoelectric autocollimator; less than $\pm 1''$ is achieved. We then put the autocollimator bounded with a corner cube inside a temperature-controlled cabinet. Figure 9(b) shows the angle drift when the temperature changes from −40 to 60 °C, while at every temperature point the error remains at an average value of less than $\pm 1''$.

The performance of the CCD photoelectric autocollimator presented here may be improved further if the devices for heat insulation and shock absorption are used to diminish external interferences. A real-time angle measuring system can also be realized if a higher-speed electronic processing system is adopted.

In conclusion, a compact and robust CCD photoelectric autocollimator with commercial off-the-shelf components is designed. The influence of the outdoor environment on the SNR and imaging quality of the measuring system is experimentally analyzed. The PWM technology and FPS methods are proposed to achieve good SNR and high measuring accuracy. Experimental results show that, when the temperature varies between −40 and 60 °C in the entire $\pm 3\,600''$ measurement range and 0.5-m measuring distance, the autocollimator has perfect linearity, $0.2''$ resolution, and $\pm 1''$ measurement accuracy. The measuring stability, dynamic range, and accuracy of the CCD photoelectric autocollimator all improve, allowing the CCD photoelectric autocollimator to be used both in laboratory and field conditions. These technologies can also be easily extended to two-dimensional CCD photoelectric autocollimators and similar situations.

The work was supported by the Shanghai Rising-Star Program (No. 09QB1400700), the Natural Science Foundation of Shanghai (No. 09ZR1435200), and the Key Basic Research Projects of Shanghai (No. 09JC1414800).

References

1. P. Martinelli, S. Musazzi, and U. Perini, Rev. Sci. Instr. **65,** 1012 (1994).
2. J. Zhang, T. Fan, and X. Cao, Proc. SPIE **6723,** 672315 (2007).
3. L. Kremer, D. Budelsky, D. Platte, and P. Von Brentano, Appl. Opt. **34,** 4827 (1995).
4. B. Li, M. Wei, B. Ye, and Q. Song, Opt. Technol. (in Chinese) **32,** 3 (2006).
5. J.Yuan, X. Long, and K. Yang, Rev. Sci. Instr. **76,** 125106 (2005).
6. Newport, "LDS-Vector Electronic Autocollimator User's Manual", http://search.newport.com/?q=*&x2=sku&q2=LDS-VECTOR.
7. Q. Li, L. Gao, and L. Chen, Opto-Electron. Eng. (in Chinese) **26,** 22 (1999).
8. Y. Lin, P. Zhang, and M. Zhao, Aviation Precision Manufacturing Technol. (in Chinese) **37,** 35 (2001).
9. H. Canabal, J. Alonso, and E. Bernabeu, Opt. Eng. **40,** 2517 (2001).
10. Y. Morimoto and M. Fujisawa, Opt. Eng. **33,** 3709 (1994).
11. W. Chen, H. Yang, X. Su, and S. Tan, Opt. Eng. **38,** 1029 (1999).
12. M. Balci and H. Foroosh, IEEE Trans. Image Proc. **15,** 1965 (2006).
13. J. Yuan and X. Long, Rev. Sci. Instr. **74,** 1362 (2003).
14. Texas Instruments, "TMS320F2812 Data Manual", http://focus.ti.com/docs/prod/ folders/print/tms320f2812.html.
15. X. Ding, Y. Li, Q. Yu, and W. Feng, Acta Opt. Sin. (in Chinese) **28,** 99 (2008).
16. M. Gao, Z. Bian, Z. Dong, Z. Fang, and R. Qu, Infra. Laser Eng. (in Chinese) **39,** 892 (2010).
17. J. Fillard, J. Lussert, M. Castagne, and H. M'timet, Signal Proc.: Image Communication **6,** 281 (1994).
18. M. R. Shortis, T. A. Clarke, and T. Short, Proc. SPIE **2350,** 239 (1994).
19. T. Chen and H. Lu, Acta Opt. Sin. (in Chinese) **22,** 1396 (2002).
20. B. Yuan, H. Yan, X. Cao, and B. Lin, Chin. Opt. Lett. **5,** 278 (2007).
21. Q. Kemao, Appl. Opt. **43,** 2695 (2004).
22. H. So, IEEE Trans. Instr. Measure. **54,** 2501 (2005).
23. J. P. Fillard, Opt. Eng. **31,** 2465 (1992).
24. J. P. Fillard, H. M'timet, J. M. Lussert, and M. Castagne, Opt. Eng. **32,** 2936 (1993).
25. Y. Wu and Q. Yu, Proc. SPIE **6027,** 60271Q (2006).
26. C. Chou, L. Y. Chou, C. K. Peng, Y. C. Huang, and K. C. Fan, Inter. J. Mach. Tools Manu. **37,** 579 (1997).